

Protocol for Precise Field Sensing in the Optical Domain with Cold Atoms in a Cavity

Robert J. Lewis-Swan,^{1,2} Diego Barberena,^{1,2} Juan A. Muniz¹,,¹ Julia R. K. Cline,¹ Dylan Young¹,,¹
James K. Thompson,¹ and Ana Maria Rey^{1,2}

¹*JILA, NIST, Department of Physics, University of Colorado, Boulder, Colorado 80309, USA*

²*Center for Theory of Quantum Matter, University of Colorado, Boulder, Colorado 80309, USA*



(Received 7 October 2019; accepted 8 April 2020; published 12 May 2020)

In the context of quantum metrology, optical cavity-QED platforms have primarily been focused on the generation of entangled atomic spin states useful for next-generation frequency and time standards. Here, we report a complementary application: the use of optical cavities to generate nonclassical states of light for electric field sensing below the standard quantum limit. We show that cooperative atom-light interactions in the strong collective coupling regime can be used to engineer generalized atom-light cat states which enable quantum enhanced sensing of small displacements of the cavity field even in the presence of photon loss. We demonstrate that metrological gains of 10–20 dB below the standard quantum limit are within reach for current cavity-QED systems operating with long-lived alkaline-earth atoms.

DOI: [10.1103/PhysRevLett.124.193602](https://doi.org/10.1103/PhysRevLett.124.193602)

Introduction.—The advent of quantum technologies promises to bring with it significant advances in quantum computation, simulation, and metrology, among others, by utilizing resources such as entanglement and many-body coherence to outperform classical analogs. For example, while sensors that use classical resources are bounded in their precision by the standard quantum limit (SQL), by employing quantum states that are entangled or possess nonclassical correlations one can realize quantum-enhanced sensors [1] that operate with superior precision bounded by the so-called Heisenberg limit (HL). For sensors composed of N particles or probes, the HL typically bounds the sensing capability by a factor $\propto 1/\sqrt{N}$ lower than the SQL [2–7].

In the optical domain, development of quantum-enhanced sensors using atom-light interactions in cavity-QED systems has concentrated on the creation of entangled atomic states through processes where the optical electromagnetic field is essentially only a mediator of interactions between atoms [8–12]. This contrasts with microwave cavities, where atom-light interactions have been used to generate nonclassical states of the field. Example platforms include Rydberg atoms [13,14], superconducting qubits [15], and trapped ions [16,17], with potential sensing applications that include the detection of single electrons [18] and photons [19], searches for dark matter [20], and quantum information processing [21]. In this work, inspired by developments in the microwave domain, we describe a protocol that realizes quantum-enhanced sensing of optical electromagnetic fields.

The generation of nonclassical states for quantum-enhanced sensing using the matter-light interaction in single qubit systems requires experiments to operate in

the strong coupling regime, achieved when the matter-light coupling rate $2g$ is larger than the decay rates of the qubit γ and the cavity κ [22–24]. While this is feasible in the microwave domain, it can be hard to attain in state-of-the-art optical cavities. Here, we demonstrate that even when $g \ll \kappa$, the interrogation of a collective ensemble coupled to a single cavity mode can be used for the preparation of generalized atom-light cat states and quantum-enhanced sensing of electromagnetic fields in the optical regime. We propose to characterize weak optical fields by sensing them as small coherent displacements of the state of the cavity mode. Although optimal detection of this perturbation of the cavity field is typically technically challenging, we discuss an interferometric protocol based on time reversal of the dynamics, which allows for nearly optimal metrological performance using accessible observables such as atomic inversion.

Our observations are relevant and directly applicable to state-of-the-art optical cavities coupled to optical transitions in alkaline-earth atoms, such as the narrow 1S_0 - 3P_1 transition in ^{88}Sr . We predict in this system it will be possible to reach 10–20 dB below the SQL operating with $\sim 10^5$ atoms. More broadly, our protocol is also relevant to other frequency regimes in platforms featuring similar types of collective atom-light couplings [17,25–31]. Conceptually, our protocol is also of potential interest for experiments sensing photon conversion of axionlike particles as in Refs. [32,33].

Model.—We seek to realize a dispersive atom-light coupling between a single mode of an optical cavity and an ensemble of atoms each encoding a spin-1/2 degree of freedom in an optical transition [Fig. 1(a)], described by the Hamiltonian:

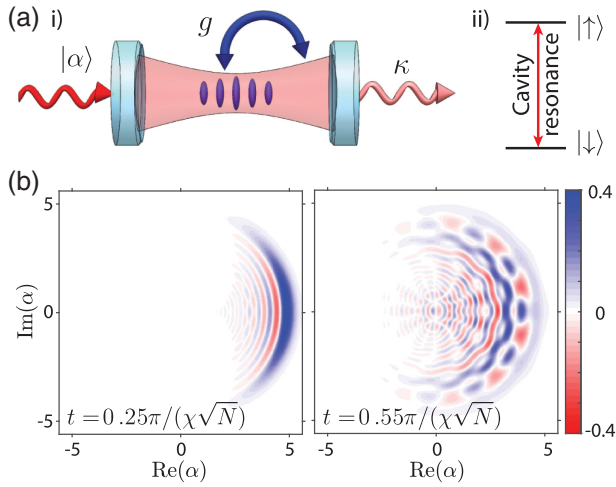


FIG. 1. (a) Proposed cavity-QED setup. N atoms are trapped in a standing-wave optical lattice. The optical transition of each atom forms a pseudospin 1/2 which is coupled to the field of the resonant optical cavity [Eq. (1)]. Photon leakage from the cavity at rate κ is the dominant decoherence mechanism. (b) Wigner function of equivalent cavity field generated by dispersive interaction, $|\phi_{\text{cav}}\rangle \propto \sum_{m=-N/2}^{N/2} c_m |\alpha e^{-i\omega_m t}\rangle$, where c_m are adopted from a coherent spin state [see Eq. (2)] and $\omega_m = \chi m$. Increasingly fine structure emerges in the phase-space distribution as time proceeds. We choose $N = 10$ and $\alpha = 4$ for illustration.

$$\hat{H} = \chi \hat{a}^\dagger \hat{a} \hat{S}_x. \quad (1)$$

Here, \hat{a} (\hat{a}^\dagger) are destruction (creation) operators for the cavity mode, $\hat{S}_{x,y,z} = \sum_{j=1}^N (\hat{\sigma}_{x,y,z}^j / 2)$ are collective spin operators with $\hat{\sigma}_{x,y,z}^j$ Pauli operators acting on atom j , and we set $\hbar = 1$ throughout this Letter. This interaction is a generalization of that commonly engineered in microwave cavity and circuit-QED platforms [22,23,34,35] and similar to that engineered in optomechanics [30]. While decoherence will play a role in any practical realization, we will first focus on the nonclassical states which can ideally be generated via the coherent dynamics described by Eq. (1). Later, we will discuss how this effective Hamiltonian can be engineered in an optical cavity, by injecting a large coherent displacement into the cavity tuned to be resonant with the atomic transition [Fig. 1(a)].

The dispersive atom-light interaction can be interpreted as an \hat{S}_x -dependent rotation of the cavity field, or alternatively generates a precession of the collective spin at a rate controlled by the cavity occupation. The former understanding motivates its use in the generation of entangled cat states composed of superpositions of bosonic coherent states, as has previously been demonstrated in the case of single Rydberg atoms in a microwave cavity [13]. In our system, we consider an initial state which is the direct product of a coherent spin state polarized along $-\hat{z}$ and a coherent state of the cavity field, $|\psi_0\rangle = |(-N/2)_z\rangle \otimes |\alpha\rangle$, where $\hat{S}_z |(-N/2)_z\rangle = (-N/2) |(-N/2)_z\rangle$ and $\hat{a}|\alpha\rangle = \alpha|\alpha\rangle$.

Time evolution of this initial state under Eq. (1) generates the superposition

$$|\psi_{\text{cat}}^{\text{AL}}\rangle = \sum_{m=-N/2}^{N/2} c_m |m_x\rangle \otimes |\alpha e^{-i\omega_m t}\rangle, \quad (2)$$

where $\omega_m = \chi m$, c_m are the expansion coefficients of the state $|(-N/2)_z\rangle$ in the basis $\hat{S}_x |m_x\rangle = m_x |m_x\rangle$, and the superscript AL emphasizes that the state is a generalized cat state of *both* the atoms and light. Generalized cat states are known to be an excellent resource for quantum metrology due to their fine structure in phase space [5,36], inversely proportional to the characteristic separation of the coherent amplitudes $\sim 1/|\alpha|$, which makes a perturbed state rapidly orthogonal to the initial cat. This is illustrated in Fig. 1(b), where we plot the Wigner function of the equivalent generalized cat state associated with just the bosonic degree of freedom, $|\phi_{\text{cav}}\rangle \propto \sum_{m=-N/2}^{N/2} c_m |\alpha e^{-i\omega_m t}\rangle$. The Wigner function displays increasing detail as the superposed coherent states $|\alpha e^{-i\omega_m t}\rangle$ disperse in time.

Quantitatively, the metrological utility of the state $|\psi_{\text{cat}}^{\text{AL}}\rangle$ to small displacements $\beta \equiv |\beta|e^{i\theta}$ is characterized by the quantum Fisher information (QFI) $\mathcal{F}_Q^\theta = 4\langle(\Delta\hat{X}_\theta)^2\rangle$. Here, $\hat{X}_\theta = \hat{a}e^{-i\theta} + \hat{a}^\dagger e^{i\theta}$ is a bosonic quadrature operator which generates the displacement and $\langle(\Delta\hat{X}_\theta)^2\rangle \equiv \langle\hat{X}_\theta^2\rangle - \langle\hat{X}_\theta\rangle^2$ its variance. The QFI is related to the sensitivity $\delta\beta$ by the quantum Cramer-Rao bound [37] $(\delta\beta)^2 \geq 1/\mathcal{F}_Q^\theta$. For short times, $t \ll 1/(|\chi|\sqrt{N})$, the QFI is maximal for displacements parallel to the initial coherently displaced state α , i.e., $\theta = 0$, and is given by $\mathcal{F}_Q^0 \approx 4(1 + N\chi^2|\alpha|^2 t^2)$ or, equivalently, $(\delta\beta)^2 \geq 1/[4(1 + N\chi^2|\alpha|^2 t^2)]$. For comparison, in this context the SQL is defined as the sensitivity achievable with the original coherent state $|\alpha\rangle$, $(\delta\beta)^2 = 1/4$. A key aspect of the metrological gain provided by a generalized cat state is the characteristic growth rate of \mathcal{F}_Q^0 , which is both collectively enhanced $\propto \sqrt{N}$ and increases with the coherent amplitude $\propto |\alpha|$. At longer times $\chi t \gtrsim 1/\sqrt{N}$, the atomic fluctuations will superpose the bosonic coherent state completely about a circle of radius $|\alpha|$ in phase space [Fig. 2(a)]. This state is sensitive to perturbations along any direction with $\mathcal{F}_Q^\theta \approx 4 + 8|\alpha|^2$.

It is useful to contrast the sensitivity achievable when measuring displacements as opposed to, e.g., phase shifts ϕ , which are also commonly encountered in optical metrology. For the latter, the SQL scales as $(\delta\phi)^2 \propto 1/\bar{n}$ for an average of \bar{n} uncorrelated particles, while the HL leads to an improved scaling of $\propto 1/\bar{n}^2$ [2–7]. In contrast, the SQL for displacements (quoted above) is independent of \bar{n} , while the HL is $\propto 1/\bar{n}$. The different scaling can be reconciled using $\bar{n} = |\alpha|^2$ and the relation $(\delta\beta)^2 \equiv (|\alpha|\delta\phi)^2$ [36].

Protocol.—While the QFI bounds the optimal sensitivity achievable with a given quantum state, in practice the

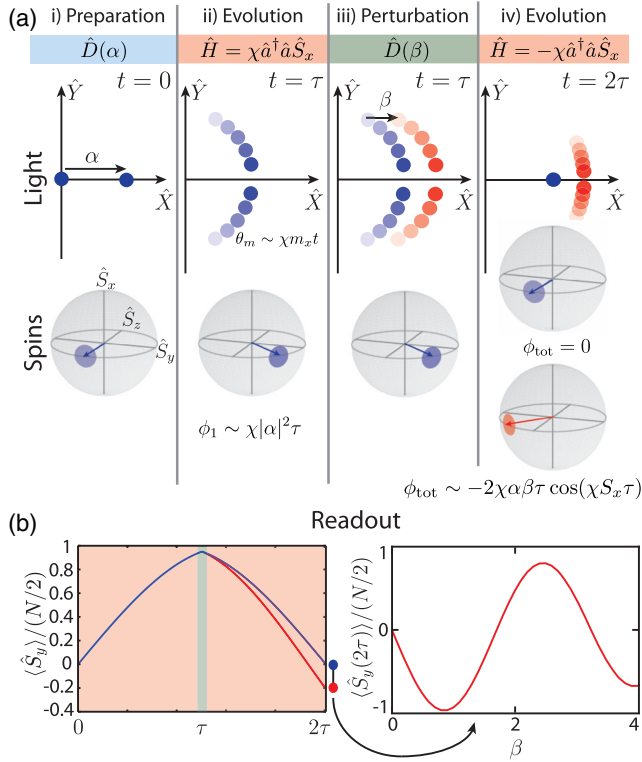


FIG. 2. (a) Preparation of generalized cat state $|\psi_{\text{cat}}^{\text{AL}}\rangle$ and interferometric protocol. (i) The cavity is injected with a coherent field α and the collective spin is fully polarized along $-\hat{z}$ (blue circles). (ii) Fluctuations in the spin projection combined with the dispersive interaction drive a rotation of the initial bosonic coherent state into a superposition at angles $\theta_m \sim \chi m_x \tau$. Conversely, the large cavity occupation rotates the collective Bloch vector by $\phi_1 \sim \chi |\alpha|^2 \tau$ about \hat{x} . (iii) The cavity field is coherently displaced by β (red circles). The spin degree of freedom is unaffected. (iv) Flipping the sign of the dispersive interaction unwinds the initial rotations. If $\beta \neq 0$, the final cavity state (red circles) does not return to the original coherent state. Similarly, the collective spin rotates back under the evolution by $\phi_2 \sim -\chi |\alpha e^{-i\chi S_x \tau} + \beta| \tau$ about \hat{x} , leading to an overall residual rotation $\phi_{\text{tot}} = \phi_1 + \phi_2 \sim -2\chi\alpha\beta\tau \cos(\chi S_x \tau)$. (b) In the absence of a displacement the time reversal revives the initial state (blue). However, perturbation of the cavity field destroys this revival, reflected in $\langle \hat{S}_y \rangle \neq 0$ for $\beta \neq 0$ (red). The dependence of the final $\langle \hat{S}_y \rangle$ on β allows the parameter β to be inferred.

sensitivity is limited by the measurements which can be implemented in the experimental platform [38]. Specifically, the phase-space structure of cat states like $|\psi_{\text{cat}}^{\text{AL}}\rangle$ [Fig. 1(b)], which makes them sensitive to displacements, also requires complex measurements necessitating single-particle resolution [39] or the ability to perform state tomography [5,36]. Predictably, then, measurements of simple cavity observables like the quadrature $\hat{X} = \hat{a} + \hat{a}^\dagger$ are not useful to sense the small perturbation of $|\psi_{\text{cat}}^{\text{AL}}\rangle$. Recently, it has been demonstrated that a powerful solution is to use a time-reversal protocol [3,12,13,17,40–47], wherein the initial

entangling dynamics are reversed after the perturbation. If the initial prepared state is Gaussian, such as $|(-N/2)_z\rangle \otimes |\alpha\rangle$ used here, then even simple observables can typically be used to achieve almost ideal sensitivity to the perturbation. Moreover, reversal protocols can have other favorable properties including robustness to experimental detection noise [43,48–50].

Our proposed interferometric protocol consists of the following steps (see Fig. 2): (1) prepare the cavity in a coherent state of real amplitude α and with pseudospin pointing along $-\hat{z}$, (2) evolve with \hat{H} for time τ , (3) coherently displace the cavity by β , (4) evolve with $-\hat{H}$ for time τ , and (5) measure an observable \hat{M} (at final time 2τ). We will demonstrate that measuring spin observables, e.g., $\hat{M} = \hat{S}_y$, is sufficient to nearly saturate the quantum Cramer-Rao bound. For completeness, other measurements such as the occupation or quadratures of the cavity field are not sensitive observables.

Physical intuition for the protocol and the choice of $\hat{M} = \hat{S}_y$ can be gained from a semiclassical picture (see Fig. 2). The first evolution can be interpreted as a rotation of the collective spin about \hat{x} by an angle $\phi_1 \sim \chi |\alpha|^2 \tau$, driven by the large coherent field in the cavity. After the perturbation of the cavity field, the reverse evolution counterrotates the spin by $\phi_2 \sim -\chi |\alpha e^{-i\chi S_x \tau} + \beta|^2 \tau$, where the phase of the α term accounts for the evolution of the bosonic mode in the first stage and S_x is a semiclassical fluctuation of characteristic scale $\sim \sqrt{N}$ due to quantum projection noise. Coarsely, this second rotation overcompensates for the first, leading to a small net rotation, $\phi_{\text{tot}} = \phi_1 + \phi_2 \sim -2\chi\alpha\beta\tau \cos(\chi S_x \tau)$, of the collective spin. The β dependence is amplified by the coherent amplitude α . Finally, measuring $\hat{M} = \hat{S}_y$ we find an attainable sensitivity,

$$(\delta\beta)^2 = \frac{\langle (\Delta \hat{M})^2 \rangle}{|\partial_\beta \langle \hat{M} \rangle|^2} \approx \frac{1}{4N\chi^2\tau^2\alpha^2}, \quad (3)$$

where we assume $\beta \rightarrow 0$ and $\tau \lesssim (\chi\sqrt{N})^{-1}$. The divergence at early times is a consequence of the spin projection noise $\langle (\Delta \hat{S}_y)^2 \rangle \propto N/4$: The atom-cavity interaction must be sufficiently long so that the rotation of the collective spin is resolvable in \hat{S}_y above the spin projection noise, $\delta S_y \equiv (N/2)\phi_{\text{tot}} = \chi\alpha\delta\beta\tau \geq \sqrt{N/4}$. In fact, this requirement can be used to qualitatively derive Eq. (3).

Engineered atom-light interaction.—The dispersive interaction, Eq. (1), can be engineered via two approaches, both starting from the underlying Tavis-Cummings model, which describes the uniform coupling of a single bosonic mode to a collection of N two-level atoms:

$$\hat{H}_{\text{TC}} = g(\hat{a}^\dagger \hat{S}^- + \hat{a} \hat{S}^+) - \Delta_c \hat{a}^\dagger \hat{a}. \quad (4)$$

Here, $2g$ is the single-photon Rabi frequency and Δ_c is the detuning of the cavity mode from the atomic transition.

We highlight that this Hamiltonian could also be realized by driving the sideband transition in a trapped ion array with uniform coupling to a single motional mode [25,51].

The most obvious method to engineer the dispersive interaction is to follow the approach used in microwave cavity platforms and work in the limit of a large detuning, $|\Delta_c| \gg |g|\sqrt{N}$. However, such a large detuning leads to an unfavorable scaling of the coherent interaction $\propto \chi\sqrt{N}$ relative to typical cavity loss rates.

Here, we instead outline a protocol to engineer a dispersive coupling by tuning the cavity to resonance $\Delta_c = 0$ [13] and injecting a large coherent state $\langle \hat{a}^\dagger \hat{a} \rangle = |\alpha|^2 \gg 1$. While to leading order this generates rapid Rabi flopping on the atomic transition, we show that the next-order correction is a dispersive atom-light interaction. To elucidate this, we adopt a number-phase representation $\hat{a} = \sqrt{\hat{a}^\dagger \hat{a}} e^{i\hat{\phi}}$ [52], and argue that the large occupation of the initial coherent state implies that the phase fluctuations $\delta\hat{\phi} \sim 1/|\alpha|$ are small with respect to number fluctuations $\delta\hat{n} = \hat{a}^\dagger \hat{a} - |\alpha|^2 \sim |\alpha|$. Moreover, we assume that these phase fluctuations remain small throughout the protocol, which is satisfied for the situations we consider here. Continuing, we approximate $\hat{a} \rightarrow \sqrt{|\alpha|^2 + \delta\hat{n}} \rightarrow |\alpha| + \delta\hat{n}/(2|\alpha|)$, keeping terms of first order in $\delta\hat{n}$. Manipulation of \hat{H}_{TC} under this approximation yields

$$H_R = g|\alpha|\hat{S}_x + \frac{g}{|\alpha|}\hat{S}_x\hat{a}^\dagger\hat{a}. \quad (5)$$

The first term and mean-field contribution $\propto |\alpha|^2$ of the second term describe the expected Rabi flopping. The dispersive coupling, equivalent to Eq. (5) with $\chi = g/|\alpha|$, is a result of our more detailed treatment incorporating quantum fluctuations. We expect this expansion to be valid when $\delta\hat{n} \ll \langle \hat{a}^\dagger \hat{a} \rangle$. More concretely, as the atom-light interaction in \hat{H}_{TC} can facilitate an exchange of up to N excitations between the bosonic and spin degrees of freedom, we require $N \ll |\alpha|^2$. Lastly, the sign of the Hamiltonian \hat{H}_R can be reversed by a global rotation about \hat{z} , so that $\hat{S}_x \rightarrow -\hat{S}_x$ and $\hat{S}_y \rightarrow -\hat{S}_y$.

Effects of dissipation.—Of concern to any realistic quantum sensor is a complete characterization of sources of technical noise and decoherence, and their effects on the sensor's performance. For our system, intrinsic sources of decoherence are photon loss from the cavity at rate κ and single-particle spontaneous emission of the atoms at rate γ . The former mechanism is important in optical cavities where typically $g \ll \kappa$. This contrasts with microwave cavities, which can operate in a strong coupling limit with a single qubit [22,23]. In the following, we demonstrate that decoherence in an optical cavity can still be overcome by harnessing the collective enhancement of an N atom ensemble.

Decoherence due to leakage of photons, at a rate $\kappa \sim 0.1$ – 1 MHz in state-of-the-art experiments [11,53–55], can be estimated from a toy model based on the archetypal

bosonic cat state $|\psi_{\text{cat}}\rangle = (|\alpha_0\rangle + |-\alpha_0\rangle)/\sqrt{2}$. Photon loss destroys the superposition (off-diagonal coherences) exponentially with the separation $|\alpha_0|$ of the coherences, $e^{-2\kappa|\alpha_0|^2 t}$. This characteristic decay is similarly displayed by the QFI with respect to small displacements, $\mathcal{F}_Q^B \approx 4 + 16|\alpha_0|^2 e^{-\kappa t} e^{-4\kappa|\alpha_0|^2 t}$ [56].

While the exponential decay of this toy model indicates that the generalized atom-light cat state is fragile, we find there is a relatively large region of parameter space in which the effects of dissipation, though negative, are not overtly detrimental to our protocol. Specifically, as entanglement and coherences are generated (via Hamiltonian evolution) simultaneously with photon loss, for an initially unentangled product state we expect that there is an optimum time at which \mathcal{F}_Q^0 is maximized. As an estimate we simplify Eq. (2) by considering the relevant coherent state amplitudes to be those that are entangled with spin components $|m_x| < \sqrt{N}$, with a dynamically evolving cat separation $\alpha_0 \approx \chi\sqrt{N}at$. Plugging this into the QFI prediction of $|\psi_{\text{cat}}\rangle$, assuming $\kappa t \ll 1$, and minimizing over t , we obtain

$$(\mathcal{F}_Q^0)_{\text{opt}} - 4 \sim \left(\frac{\chi^2 \alpha^2 N}{\kappa^2}\right)^{1/3}, \quad t_{\text{opt}} \sim \left(\frac{1}{\kappa \chi^2 N \alpha^2}\right)^{1/3}. \quad (6)$$

Even if $\chi \ll \kappa$, as is typical in optical systems, Eq. (6) indicates that $\chi|\alpha|\sqrt{N} > \kappa$ is sufficient to obtain a meaningful QFI. This estimated scaling is borne out in the sensitivity achievable with collective spin measurements: For $\kappa\tau \ll 1$, the sensitivity is [56]

$$(\delta\beta)_\kappa^2 \approx \frac{1 + \frac{2}{3}\kappa(\sqrt{N}\chi|\alpha|\tau)^2\tau}{4N\chi^2|\alpha|^2\tau^2} = \frac{1}{4N\chi^2|\alpha|^2\tau^2} + \frac{\kappa\tau}{6}, \quad (7)$$

which has the optimum

$$(\delta\beta)_{\kappa,\text{opt}}^2 = \frac{1}{4} \left(\frac{3\kappa^2}{\chi^2 N \alpha^2}\right)^{1/3}, \quad \tau_{\text{opt}} = \left(\frac{3}{\kappa \chi^2 N \alpha^2}\right)^{1/3}. \quad (8)$$

This shows identical scaling to the quantum Cramer-Rao bound $1/(\mathcal{F}_Q^0)_{\text{opt}}$. For our scheme $\chi = g/|\alpha|$, so the α factors cancel but N -fold enhancement remains, $(\delta\beta)_{\kappa,\text{opt}}^2 = (1/4)[3\kappa^2/(g^2N)]^{1/3}$. This grants some freedom to tune α to guarantee the validity of Eq. (5).

For state-of-the-art experiments using long-lived optical transitions $\gamma \ll \kappa$, and spontaneous emission leads predominantly to a single-particle decay of spin observables on timescales $1/\gamma$ [56]. Given that $\tau_{\text{opt}} \ll 1/\gamma$, we can neglect spontaneous emission in our analysis.

Experimental realization.—For concreteness, we present an example calculation for the optical cavity described in Refs. [53,58], where a single cavity mode is resonantly coupled to an ensemble of N atoms trapped in a standing-wave optical lattice oriented along the cavity axis. We assume uniform coupling of the atoms to the cavity mode, which can be realized via site-selective loading in

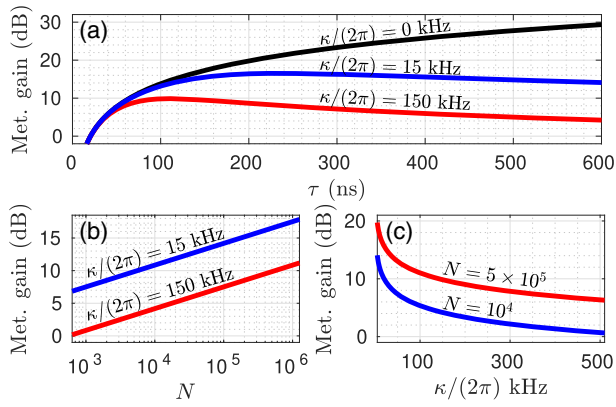


FIG. 3. (a) Metrological gain $(\delta\beta)_{\text{SQL}}^2/(\delta\beta)^2 \equiv [4(\delta\beta)^2]^{-1}$ as a function of interaction time τ , for a range of cavity decay rates κ . The cavity is coupled resonantly, $N = 5 \times 10^5$, $\alpha = 100\sqrt{N}$, and $g/(2\pi) = 11$ kHz, for the $^1S_0 \rightarrow ^3P_1$ transition of ^{88}Sr . Optimal gain (maximized over τ) is also plotted for (b) N and (c) κ .

the spatial lattice or using a ring cavity. Relevant experimental parameters are $N \sim 10^5$ – 10^6 atoms, $\alpha = 100\sqrt{N}$, and $g/(2\pi) = 11$ kHz for the $^1S_0 \rightarrow ^3P_1$ transition in ^{88}Sr [53,58]. Preparation of the initial spin state $|(-N/2)_z\rangle$ is via optical pumping to the 1S_0 ground state, while the coherent state $|\alpha\rangle$ is injected via a laser. The spin projection \hat{S}_y is mapped into atomic inversion \hat{S}_z by global rotations and measured by fluorescence [53]. In Fig. 3(a) we show the metrological gain over the SQL for $\kappa/(2\pi) = (0, 15, 150)$ kHz. We predict improved sensitivity of at least 10 dB beyond the SQL for $\kappa/(2\pi) = 150$ kHz and $N = 5 \times 10^5$.

Conclusion.—We have demonstrated that atom-light interactions in an optical cavity can be utilized to generate nonclassical states for quantum metrology in the optical domain. While the examples presented in this work focused on optical cavities, our methods can be readily applied to other systems including trapped ions [25], microwave cavities [26], circuit QED [27,28], and hybrid quantum systems [29,30], with immediate applications to the sensing of weak forces [17,31].

We acknowledge helpful discussions with J. J. Bollinger, B. Brubaker, K. Gilmore, and M. A. Perlin during the preparation of this manuscript. This work is supported by the AFOSR Grant No. FA9550-18-1-0319, by the DARPA and ARO Grant No. W911NF-16-1-0576, the ARO single investigator award W911NF-19-1-0210, the NSF PHY1820885, NSF JILA-PFC PHY-1734006 grants, and by NIST.

[1] C. L. Degen, F. Reinhard, and P. Cappellaro, *Rev. Mod. Phys.* **89**, 035002 (2017).
 [2] C. M. Caves, K. S. Thorne, R. W. P. Drever, V. D. Sandberg, and M. Zimmermann, *Rev. Mod. Phys.* **52**, 341 (1980).

[3] B. Yurke, S. L. McCall, and J. R. Klauder, *Phys. Rev. A* **33**, 4033 (1986).
 [4] M. J. Holland and K. Burnett, *Phys. Rev. Lett.* **71**, 1355 (1993).
 [5] W. H. Zurek, *Nature (London)* **412**, 712 (2001).
 [6] V. Giovannetti, S. Lloyd, and L. Maccone, *Phys. Rev. Lett.* **96**, 010401 (2006).
 [7] L. Pezzè, A. Smerzi, M. K. Oberthaler, R. Schmied, and P. Treutlein, *Rev. Mod. Phys.* **90**, 035005 (2018).
 [8] H. Ritsch, P. Domokos, F. Brennecke, and T. Esslinger, *Rev. Mod. Phys.* **85**, 553 (2013).
 [9] M. H. Schleier-Smith, I. D. Leroux, and V. Vuletić, *Phys. Rev. Lett.* **104**, 073604 (2010).
 [10] K. C. Cox, G. P. Greve, J. M. Weiner, and J. K. Thompson, *Phys. Rev. Lett.* **116**, 093602 (2016).
 [11] B. Braverman, A. Kawasaki, E. Pedrozo-Peñafiel, S. Colombo, C. Shu, Z. Li, E. Mendez, M. Yamoah, L. Salvi, D. Akamatsu, Y. Xiao, and V. Vuletić, *Phys. Rev. Lett.* **122**, 223203 (2019).
 [12] O. Hosten, R. Krishnakumar, N. J. Engelsen, and M. A. Kasevich, *Science* **352**, 1552 (2016).
 [13] M. Penasa, S. Gerlich, T. Rybarczyk, V. Métillon, M. Brune, J. M. Raimond, S. Haroche, L. Davidovich, and I. Dotsenko, *Phys. Rev. A* **94**, 022313 (2016).
 [14] A. Facon, E.-K. Dietsche, D. Grosso, S. Haroche, J.-M. Raimond, M. Brune, and S. Gleyzes, *Nature (London)* **535**, 262 (2016).
 [15] B. Vlastakis, G. Kirchmair, Z. Leghtas, S. E. Nigg, L. Frunzio, S. M. Girvin, M. Mirrahimi, M. H. Devoret, and R. J. Schoelkopf, *Science* **342**, 607 (2013).
 [16] K. C. McCormick, J. Keller, S. C. Burd, D. J. Wineland, A. C. Wilson, and D. Leibfried, *Nature (London)* **572**, 86 (2019).
 [17] S. C. Burd, R. Srinivas, J. J. Bollinger, A. C. Wilson, D. J. Wineland, D. Leibfried, D. H. Slichter, and D. T. C. Allcock, *Science* **364**, 1163 (2019).
 [18] M. H. Devoret and R. J. Schoelkopf, *Nature (London)* **406**, 1039 (2000).
 [19] C. Hempel, B. P. Lanyon, P. Jurcevic, R. Gerritsma, R. Blatt, and C. F. Roos, *Nat. Photonics* **7**, 630 (2013).
 [20] M. Malnou, D. A. Palken, B. M. Brubaker, L. R. Vale, G. C. Hilton, and K. W. Lehnert, *Phys. Rev. X* **9**, 021023 (2019).
 [21] T. D. Ladd, F. Jelezko, R. Laflamme, Y. Nakamura, C. Monroe, and J. L. O’Brien, *Nature (London)* **464**, 45 (2010).
 [22] D. I. Schuster, A. A. Houck, J. A. Schreier, A. Wallraff, J. M. Gambetta, A. Blais, L. Frunzio, J. Majer, B. Johnson, M. H. Devoret, S. M. Girvin, and R. J. Schoelkopf, *Nature (London)* **445**, 515 (2007).
 [23] S. M. Girvin, *Quantum Machines: Measurement and Control of Engineered Quantum Systems* (Oxford University Press, Oxford, 2014), pp. 113–256.
 [24] B. Hacker, S. Welte, S. Daiss, A. Shaukat, S. Ritter, L. Li, and G. Rempe, *Nat. Photonics* **13**, 110 (2019).
 [25] A. Safavi-Naini, R. J. Lewis-Swan, J. G. Bohnet, M. Gärtner, K. A. Gilmore, J. E. Jordan, J. Cohn, J. K. Freericks, A. M. Rey, and J. J. Bollinger, *Phys. Rev. Lett.* **121**, 040503 (2018).
 [26] S. Deléglise, I. Dotsenko, C. Sayrin, J. Bernu, M. Brune, J.-M. Raimond, and S. Haroche, *Nature (London)* **455**, 510 (2008).

- [27] J. M. Fink, R. Bianchetti, M. Baur, M. Göppl, L. Steffen, S. Filipp, P. J. Leek, A. Blais, and A. Wallraff, *Phys. Rev. Lett.* **103**, 083601 (2009).
- [28] J. J. Viennot, X. Ma, and K. W. Lehnert, *Phys. Rev. Lett.* **121**, 183601 (2018).
- [29] S. Kolkowitz, A. C. Bleszynski Jayich, Q. P. Unterreithmeier, S. D. Bennett, P. Rabl, J. G. E. Harris, and M. D. Lukin, *Science* **335**, 1603 (2012).
- [30] M. Aspelmeyer, T. J. Kippenberg, and F. Marquardt, *Rev. Mod. Phys.* **86**, 1391 (2014).
- [31] K. A. Gilmore, J. G. Bohnet, B. C. Sawyer, J. W. Britton, and J. J. Bollinger, *Phys. Rev. Lett.* **118**, 263602 (2017).
- [32] N. Du *et al.* (ADMX Collaboration), *Phys. Rev. Lett.* **120**, 151301 (2018).
- [33] L. Zhong *et al.*, *Phys. Rev. D* **97**, 092001 (2018).
- [34] P. Bertet, A. Auffèves, P. Maioli, S. Osnaghi, T. Meunier, M. Brune, J. M. Raimond, and S. Haroche, *Phys. Rev. Lett.* **89**, 200402 (2002).
- [35] A. Blais, R.-S. Huang, A. Wallraff, S. M. Girvin, and R. J. Schoelkopf, *Phys. Rev. A* **69**, 062320 (2004).
- [36] F. Toscano, D. A. R. Dalvit, L. Davidovich, and W. H. Zurek, *Phys. Rev. A* **73**, 023803 (2006).
- [37] S. L. Braunstein and C. M. Caves, *Phys. Rev. Lett.* **72**, 3439 (1994).
- [38] G. Tóth and I. Apellaniz, *J. Phys. A* **47**, 424006 (2014).
- [39] J. J. Bollinger, W. M. Itano, D. J. Wineland, and D. J. Heinzen, *Phys. Rev. A* **54**, R4649 (1996).
- [40] F. Hudelist, J. Kong, C. Liu, J. Jing, Z. Ou, and W. Zhang, *Nat. Commun.* **5**, 3049 (2014).
- [41] D. Linnemann, H. Strobel, W. Muessel, J. Schulz, R. J. Lewis-Swan, K. V. Kheruntsyan, and M. K. Oberthaler, *Phys. Rev. Lett.* **117**, 013001 (2016).
- [42] T. Macrì, A. Smerzi, and L. Pezzè, *Phys. Rev. A* **94**, 010102 (R) (2016).
- [43] E. Davis, G. Bentsen, and M. Schleier-Smith, *Phys. Rev. Lett.* **116**, 053601 (2016).
- [44] S. S. Szigeti, R. J. Lewis-Swan, and S. A. Haine, *Phys. Rev. Lett.* **118**, 150401 (2017).
- [45] F. Anders, L. Pezzè, A. Smerzi, and C. Klempt, *Phys. Rev. A* **97**, 043813 (2018).
- [46] J. Huang, M. Zhuang, B. Lu, Y. Ke, and C. Lee, *Phys. Rev. A* **98**, 012129 (2018).
- [47] J. P. Wrubel, A. Schwettmann, D. P. Fahey, Z. Glassman, H. K. Pechkis, P. F. Griffin, R. Barnett, E. Tiesinga, and P. D. Lett, *Phys. Rev. A* **98**, 023620 (2018).
- [48] S. P. Nolan, S. S. Szigeti, and S. A. Haine, *Phys. Rev. Lett.* **119**, 193601 (2017).
- [49] S. A. Haine, *Phys. Rev. A* **98**, 030303(R) (2018).
- [50] S. S. Mirkhalaf, S. P. Nolan, and S. A. Haine, *Phys. Rev. A* **97**, 053618 (2018).
- [51] J. G. Bohnet, B. C. Sawyer, J. W. Britton, M. L. Wall, A. M. Rey, M. Foss-Feig, and J. J. Bollinger, *Science* **352**, 1297 (2016).
- [52] L. Susskind and J. Glogower, *Phys. Phys. Fiz.* **1**, 49 (1964).
- [53] M. A. Norcia, R. J. Lewis-Swan, J. R. K. Cline, B. Zhu, A. M. Rey, and J. K. Thompson, *Science* **361**, 259 (2018).
- [54] E. J. Davis, G. Bentsen, L. Homeier, T. Li, and M. H. Schleier-Smith, *Phys. Rev. Lett.* **122**, 010405 (2019).
- [55] V. D. Vaidya, Y. Guo, R. M. Kroeze, K. E. Ballantine, A. J. Kollár, J. Keeling, and B. L. Lev, *Phys. Rev. X* **8**, 011002 (2018).
- [56] See Supplemental Material at <http://link.aps.org/supplemental/10.1103/PhysRevLett.124.193602> for a systematic analysis of the effects of decoherence, which includes Refs. [37,57].
- [57] D. G. O’Neill, D. B. Church, P. D. McGreevy, P. C. Thomson, and D. C. Brodbelt, *J. Feline Med. Surg.* **17**, 125 (2014).
- [58] M. A. Norcia and J. K. Thompson, *Phys. Rev. A* **93**, 023804 (2016).